Hindawi
Journal of Chemistry
Volume 2020, Article ID 3878409, 7 pages
https://doi.org/10.1155/2020/3878409

Research Article

Simple Methods to Synthesize YVO_4 Nanocrystals or Microcrystals without Any Templates or Surfactants

Baogeng Xie, Min Chen, Junyue Lin, Xiaobing Liu, Shujun Peng, and Luping Zhong

School of Chemistry and Chemical Engineering, Jinggangshan University, Ji'an 343009, China

Correspondence should be addressed to Baogeng Xie; liu34111@163.com

Received 13 August 2019; Revised 5 April 2020; Accepted 17 April 2020; Published 11 May 2020

Academic Editor: João Paulo Leal

YVO_4 crystals with different sizes and shapes were produced through hydrothermal treatment and sonication method without any surfactants or templates. X-ray powder diffraction (XRD), transmission electron microscopy (TEM), and photoluminescence (PL) were used to characterize the obtained products. YVO_4 nanocrystals with spindle-like shape had been produced through the two different treating methods. YVO_4 crystals, which are bipyramid-capped and micrometer-sized, had been obtained through a simple hydrothermal treatment. Uniform microsized cuboids had been produced through hydrothermal treatment with the final pH value = 2.5. The effects of different final pH values on the shape and crystallinity of products were studied. To determine photoluminescence performances, Eu^{3+}(5%)-doped YVO_4 nanocrystals had been synthesized through different methods in various environments and it had been confirmed that crystallinity would affect photoluminescence intensity.

1. Introduction

Rare earth orthovanadate is a kind of important oxide in materials science and technology [1–12]. And YVO_4 has wide applications in many fields, such as polarizer [13, 14] and laser host material [15, 16]. In particular, due to its high efficiency of photoluminescence, Eu^{3+}-doped YVO_4 (YVO_4:Eu) was used as a red phosphor and was used in color television cathode ray tubes [17]. Although YVO_4:Eu used as commercial phosphor is bulk material, small-scale YVO_4:Eu is expected to have unique photoluminescence performances and applications. So the study of synthesizing small-scale YVO_4 is necessary. Recently, many papers have reported different methods for producing YVO_4 nanoparticles [18–22].

Wu et al. used a hydrothermal method to synthesize rod-like, olive-like, pineapple-like, and particle-like nanocrystals of the YVO_4:(5%) Eu, respectively, and they confirmed that the olive-like nanocrystals have enhanced luminescence intensity compared with nanocrystals with other shapes [23]. Spindle-like YVO_4:(5%) Eu^{3+} nanocrystals have been synthesized with (Y, Eu) $(NO_3)_3$ and NH_4VO_3 as starting materials through sonication method by Zhu et al. They claimed that the use of ultrasonic irradiation has a remarkable effect on the morphology of the particles produced [24]. Li et al. demonstrated a hydrothermal treatment for obtaining YVO_4:(5%) Eu^{3+} nanobelts and polyhedron microcrystals with (Y, Eu) $(NO_3)_3$ and NH_4VO_3 as reacting reagents. It has been proved that the influence of pH values on the morphology of the products is essential [25].

In this paper, we report two simple routes to synthesize spindle-like YVO_4 nanocrystals with Y $(NO_3)_3$ and Na_3VO_4 as starting materials. YVO_4 microcrystals of bipyramid-capped shape and cuboids have been produced through hydrothermal treatment with different final pH values. It has been found that pH value is a key factor for influencing the morphology of products, which is consistent with the results gained by previous works. And it is also found that different morphologies of products will bring different PL intensities.

2. Experimental Section

2.1. Synthesis. All the starting materials used in this work were of analytical grade. In a typical synthesis procedure, 0.0016 mol Y $(NO_3)_3{\cdot}6H_2O$ and 0.0016 mol $Na_3VO_4{\cdot}12H_2O$ were mixed with an appropriate amount of distilled water

and immediately a white precipitate appeared. Then, 3 M HNO_3 was dripped into the obtained suspension to dissolve the white precipitate and a transparent golden yellow solution was obtained. The proper amount of 1 M NaOH was added to the solution to make the final pH at a designed value and stirred for 10 min to obtain solution precursor. Then, the solution precursor was transferred into a 100 ml Teflon-lined stainless steel autoclave for hydrothermal treatment. When the solution had been hydrothermally treated at a determined temperature for a needed time, the autoclave was cooled to room temperature naturally. And the precipitate was separated by centrifugation, washed with distilled water and absolute ethanol, and dried at room temperature for further characterization. When the samples of YVO_4 were obtained through the sonication method, the solution precursor was produced through the same process. And the solution mixture was exposed to ultrasonic irradiation in ambient air for 2 h.

2.2. Characterization. The X-ray diffraction (XRD) patterns of the samples were examined on a Japan Rigaku D/Max-γ X-ray diffractometer equipped with a rotation anode and graphite monochromatized CuKα radiation ($\lambda = 1.54178$ Å). The transmission electron microscopy (TEM) images of the as-synthesized samples were obtained on a JEOL JEM-100 CXII operated at an accelerating voltage of 100 kV. The high-resolution transmission electron microscopy (HRTEM) images were obtained on a Philips Tecnai F30 high-resolution field-emission transmission electron microscope operated at 300 kV. The samples to be measured were dispersed in absolute ethanol under vibrating in the ultrasonic pool, and then, the solutions were dropped onto a copper grid coated with amorphous carbon films and dried in air before performance. Fluorescence spectra were recorded on a Hitachi F-4500 spectrophotometer equipped with a 150 W Xe arc lamp at room temperature; the emission spectra were measured at a fixed band-pass of 0.2 nm with the same instrument parameters (5.0 nm for excitation split, 1.0 nm for emission split, and 700 V for PMT voltage).

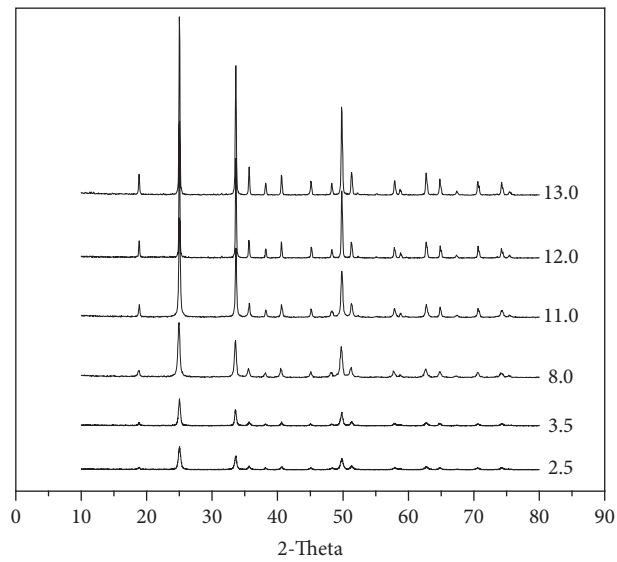

Figure 1: XRD patterns of the samples produced with different final pH values at 180°C for 24 h through hydrothermal route.

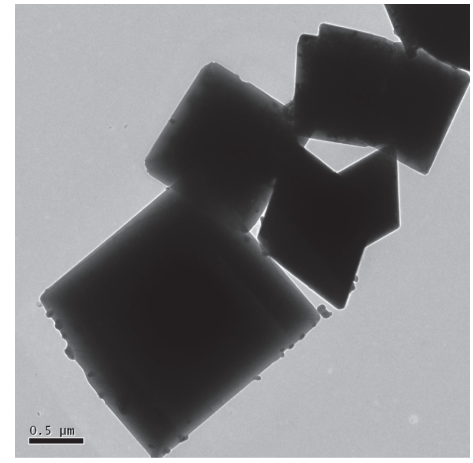

Figure 2: TEM images of YVO_4 crystals produced at pH = 2.5 through hydrothermal route.

3. Results and Discussion

XRD patterns of the produced samples are shown in Figure 1. Diffraction peaks of all the samples can be indexed to tetragonal phased YVO_4, so it can be resulted that pure tetragonal phased YVO_4 can be produced in a wide pH range through hydrothermal route. Stronger diffraction peaks appear in the products obtained in higher final pH value, which demonstrates that products of higher crystallinity are produced in higher pH surroundings.

Figure 2 provides the TEM images of YVO_4 crystals produced at pH = 2.5. It can be seen from Figure 2 that micrometer-sized cuboids have been obtained. The uniform cuboids have lengths of about 3 μm and widths of about 2 μm.

Figure 3 presents TEM images of YVO_4 nanocrystals which were produced in weakly acidic and basic environment with hydrothermal treatment at 180°C for 24 h, respectively. Figure 3 shows that uniform nanocrystals are produced in both surroundings and it can be seen that the nanocrystals have a spindle-like morphology. The spindle-like particles with an equatorial diameter of 50–70 nm and a length of 120–200 nm are produced at pH = 6.0. And when treated at pH = 9.0, spindle-like particles with a little bigger size are obtained. It is observed that the nanocrystals produced at pH = 6.0 are accumulated of many small nanorods; however, nanocrystals produced at pH = 9.0, which have higher crystallinity, are accumulated of some bigger nanorods.

TEM images of YVO_4 crystals produced at pH = 12.0 and 13.0 are presented in Figure 4. It is obvious that the pH value of the synthesis solution plays an important role in shape and size of the obtained crystals. It is shown that crystals of different shapes with bigger size are obtained in solution of higher final pH value. And it can also be observed that the

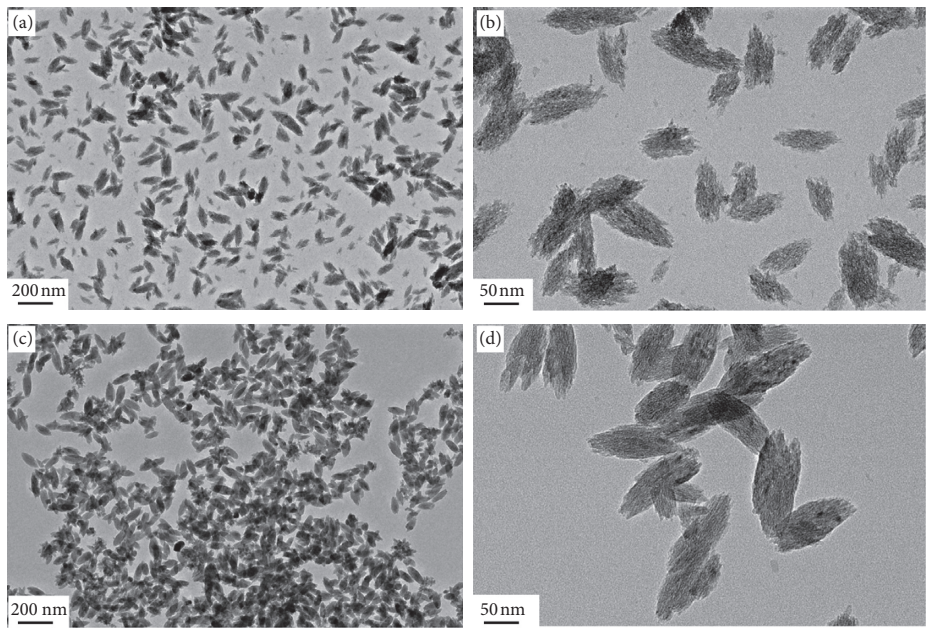

Figure 3: TEM images of YVO_4 nanocrystals produced at (a), (b) pH = 6.0, and (c), (d) pH = 9.0 through hydrothermal route.

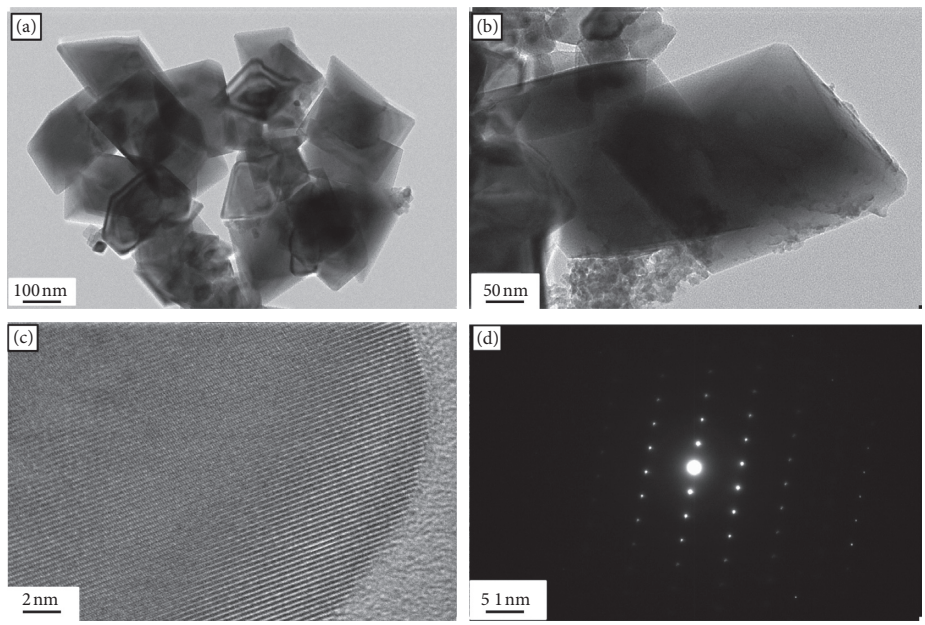

Figure 4: TEM images of YVO_4 crystals produced at (a) pH = 12.0, (b) pH = 13.0 and HRTEM image (c) and SAED (d) of crystals produced at pH = 13.0 through hydrothermal route.

shape of crystals produced at pH = 13.0 is similar to that produced at pH = 12.0; however, the size of crystals produced at pH = 13.0 is bigger. Figure 4(c) presents HRTEM image of crystals produced at pH = 13.0. It can be known from Figure 4(c) that YVO_4 of tetragonal phase is obtained, which is consistent with the result of XRD, and the obtained crystals have a high crystallinity. The selected area electron diffraction (SAED) pattern indicates that products obtained at pH = 13.0 are single crystalline.

YVO_4 nanocrystals are also obtained through the ultrasonic irradiation method with the same pretreatment of raw materials; however, it can be observed from Figure 5 that poor crystallinity was obtained when final pH value is increased to 12.0, which is different from the result of hydrothermal treatment. Typical TEM images are presented in Figures 6(c) and 6(d). Similarly to hydrothermal treatment, nanocrystals produced with the ultrasonic irradiation method are spindle-like and nanocrystals produced in the two different environments have the same size, which have equatorial diameter and length in the range of 40–50 nm and 70–120 nm, respectively. Nanocrystals produced in the two different environments are accumulated of small nanorods,

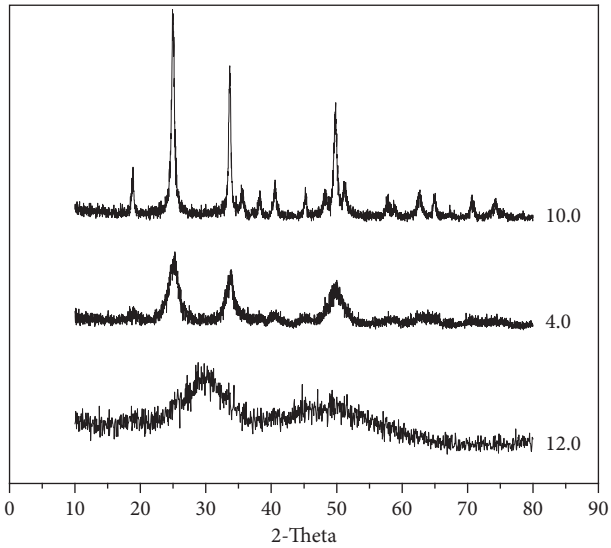

Figure 5: XRD patterns of samples produced through ultrasonic irradiation at different pH end values.

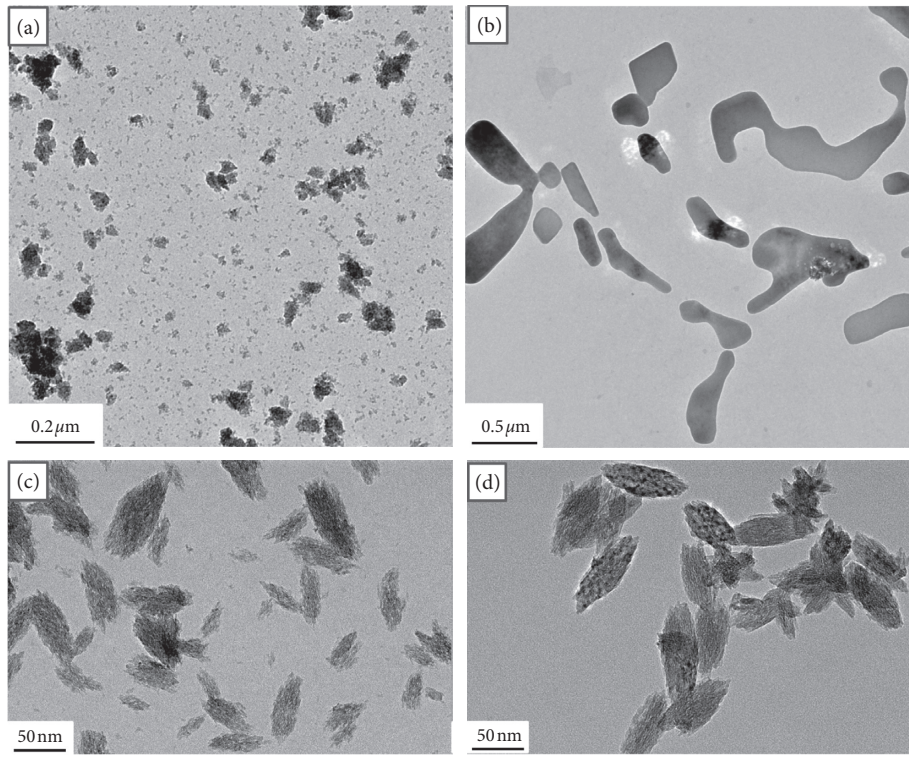

Figure 6: TEM images of YVO_4 nanocrystals produced through ultrasonic irradiation for 2 h at (a) pH = 2.5, (b) pH = 12.0, (c), pH = 6.0, and (d) pH = 9.0.

which is also similar to the result of hydrothermal treatment. So it can be presumed that the formation mechanism of YVO_4 nanocrystals obtained through the two different treatments is the same. However, the size of products obtained through the sonication method is smaller than that obtained through hydrothermal treatment, and the crystallinity of the latter is higher than the former.

Figures 6(a) and 6(b) have provided TEM images of YVO_4 nanocrystals produced through ultrasonic irradiation for 2 h at pH = 2.5 and 12.0. Uniform cuboids and bipyramid-capped crystals have not been produced through the ultrasonic irradiation method with pH = 2.5 and 12.0.

From the synthesis and characterization, it is known that there are Y^{3+}, polyvanadate, much OH^-, and precipitated YVO_4 of irregular shape existing in the precursor. The formation of YVO_4 uniform crystals is based on this reaction under hydrothermal treatment: irregular shaped $YVO_4 \longrightarrow Y^{3+}$ + polyvanadate + $OH^- \longrightarrow$ uniform shaped

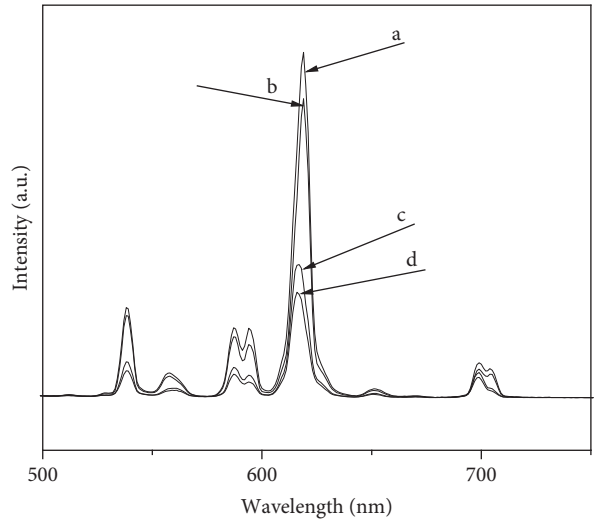

Figure 7: Emission spectra of YVO_4:(5%) Eu^{3+} produced through hydrothermal treatment with different pH end values: (a) 13.0, (b) 12.0, (c) 11.0, and (d) 8.0 under the excitation of 310 nm at room temperature.

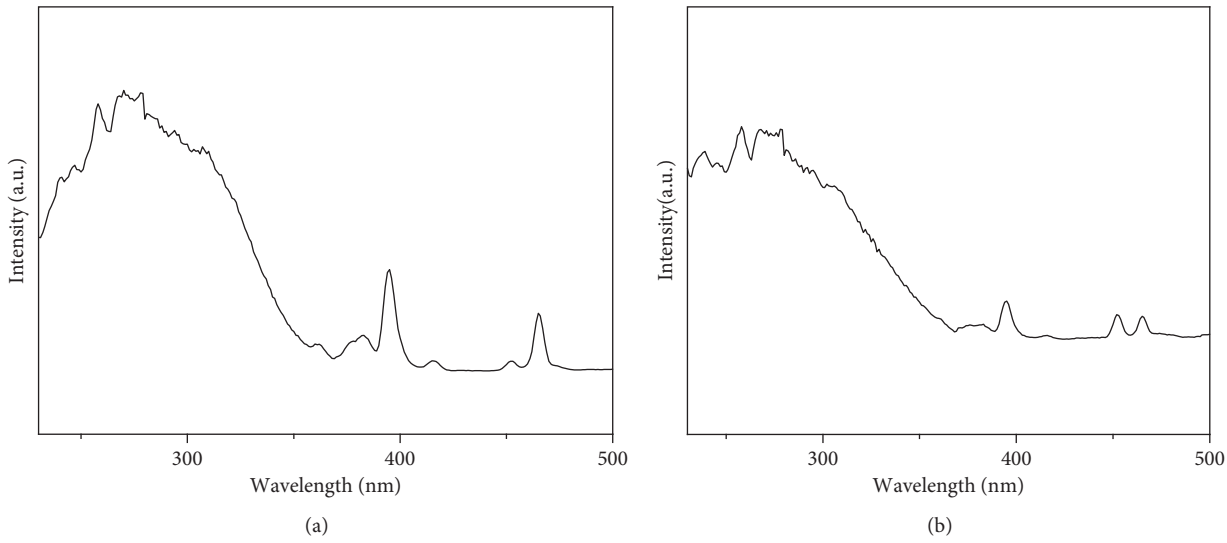

Figure 8: Excitation spectrum of YVO_4:(5%) Eu^{3+} obtained under emission of 618 nm at room temperature through (a) hydrothermal method with pH = 11 and (b) sonication method with pH 12.

YVO_4. In other words, a dissolution-reprecipitation process is provided. Here, Y^{3+} ions existing as mobile cations are gradually incorporated into the polyvanadate anions and then lead to the formation of uniform YVO_4 crystals [9]. It is obvious that the pH value plays a key role in shape selection. The [010] face is rich in Y^{3+}, so it is believed that the (010) growth direction can attract positive ions (Y^{3+}) and exclude negative ions. The (010) growth direction will be disturbed and even inhibited by OH^- when its concentration is high. When the final pH value is in the range 4.0–10, the existence of OH^- disturbs the (010) growth direction, and nanocrystals produced in this pH range show a spindle-like shape. However, when the concentration of OH^- increased and pH value achieves 13, the (010) growth direction is more inhibited and crystals produced in this environment are bipyramid-capped. When the final pH value is fixed at 2.5, the enhancement of H_3O^+ makes the face (010) and other faces grow well, and micrometer-sized cuboids are obtained.

YVO_4:(5%) Eu^{3+} products are produced through different treatments in different environments to study optical properties. It can be observed from Figure 7 that PL intensity of products obtained in basic solution is stronger than that obtained in acidic solution and PL intensity becomes weaker with decreased final pH value. Figure 8 shows the excitation spectrum of YVO_4:(5%) Eu^{3+} obtained through the hydrothermal method with pH = 11 and the sonication method with pH = 12. The excitation spectrum is obtained under the emission of 618 nm and it can be known that the biggest excitation peak is at 280 nm. It can be observed from Figure 9 that higher final pH value will bring stronger intensity at

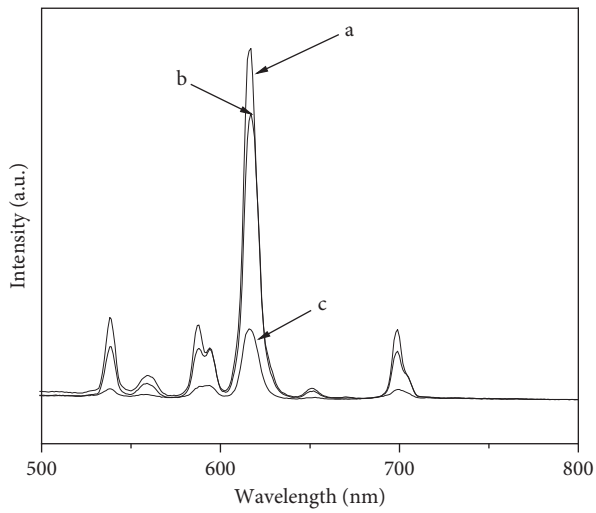

Figure 9: Emission spectra of YVO_4:(5%) Eu^{3+} produced through ultrasonic irradiation with different pH end values: (a) 10.0, (b) 8.0, and (c) 12.0 under the excitation of 280 nm at room temperature.

pH = 10. Weaker intensity is obtained when the final pH value is increased to 12 because of the absence of YVO_4. Emission spectra shown in Figure 9 are under 280 nm with 600 V for PMT voltage, which is higher than that used for products obtained through hydrothermal treatment. So it can be realized that PL intensity of products obtained through hydrothermal treatment is greatly stronger than that obtained through the sonication method. It can be presumed that the shape of products will influence optical properties and bipyramid-capped products appear greater PL intensity. Higher crystallinity will bring better photoluminescence performance, which is consistent with the previous literature.

4. Conclusions

4.1. Hydrothermal Route. In summary, YVO_4 crystals with spindle-like, bipyramid-capped, micrometer-sized cuboid shape have been produced through hydrothermal treatment. Different shapes have been obtained with different final pH values. Bipyramid-capped crystals have been produced with pH = 12.0, 13.0. And the products obtained at pH = 13.0 are single crystalline.

4.2. Ultrasonic Route. Three shapes have been obtained through sonication method: spindle-like shape, rod-like shape, and nanoparticles. The crystallinity of products obtained through hydrothermal treatment is higher than that produced through the sonication method. The pH value of the solution will affect the shape and crystallinity of products remarkably. Higher pH value will result in products of higher crystallinity.

4.3. Photoluminescence. A variety of Eu^{3+}(5%)-doped YVO_4 products have been synthesized to study their photoluminescence performances. It has been confirmed that higher pH end value will bring stronger PL intensity when the produced host material is YVO_4; however, when the pH end value is controlled at 12.0 through ultrasonic irradiation, products exhibit remarkably lower PL intensity due to the low crystallinity.

Data Availability

The data used to support the findings of this study are available from the corresponding author upon request.

Conflicts of Interest

The authors declare that they have no conflicts of interest.

Acknowledgments

This project was supported financially by the Doctoral Research Program of Jinggangshan University of China (no. JZB1813) and the Science and Technology Program of Jiangxi Provincial Education Bureau (no. GJJ180575).

References

[1] M. Yu, J. Lin, Z. Wang et al., "Fabrication, patterning, and optical properties of nanocrystalline YVO_4:A (A = Eu^{3+}, Dy^{3+}, Sm^{3+}, Er^{3+}) phosphor films via Sol–Gel soft lithography," *Chemistry of Materials*, vol. 14, no. 5, pp. 2224–2231, 2002.

[2] R. M. Mohamed, F. A. Harraz, and I. A. Mkhalid, "Hydrothermal synthesis of size-controllable Yttrium Orthovanadate (YVO4) nanoparticles and its application in photocatalytic degradation of direct blue dye," *Journal of Alloys and Compounds*, vol. 532, pp. 55–60, 2012.

[3] Z. Hou, P. Yang, C. Li et al., "Preparation and luminescence properties of YVO_4:Ln and Y (V, P) O_4: Ln (ln = Eu^{3+}, Sm^{3+}, Dy^{3+}) nanofibers and microbelts by Sol–Gel/electrospinning process," *Chemistry of Materials*, vol. 20, no. 21, pp. 6686–6696, 2008.

[4] K. V. Naveen, K. E. Neerugatti, A. S. Satyapaul, and M. Giridhar, "Cocatalyst free Z-schematic enhanced H_2 evolution over $LaVO_4$/$BiVO_4$ composite photocatalyst using Ag as an electron mediator," *Appllied Catalysis B: Environmental*, vol. 220, pp. 512–523, 2018.

[5] S. Mahaoatra, G. Madras, and T. N. G. Row, "Characterization and photocatalytic activity of lanthanide (Ce, Pr and Nd) orthovanadates," *Industrial & Engineering Chemistry Research*, vol. 46, pp. 1013–1017, 2007.

[6] L. Zong, J. Xu, S. Jiang et al., "Composite yttrium-carbonaceous spheres templated multi-shell YVO_4 hollow spheres with superior upconversion photoluminescence," *Advanced Materials*, vol. 29, no. 9, p. 1604377, 2017.

[7] D. T. Chinh, T. P. H. Phuong, M. D. D. Thi, and M. D. Chien, "Sonochemical synthesis and properties of YVO_4: Eu^{3+} nanocrystals for luminescent security ink applications," *Journal of Chemistry*, vol. 2019, Article ID 5749702, 13 pages, 2019.

[8] Y. K. Kshetri, C. Regmi, S. W. Lee, and T. H. Kim, "Microwave hydrothermal synthesis and upconversion properties of Yb^{3+}/Er^{3+} doped YVO_4 nanoparticles," *Nanotechnology*, vol. 29, no. 20, p. 282, 2018.

[9] H. Wu, H. Xu, Q. Su, T. Chen, and M. Wu, "Size- and shape-tailored hydrothermal synthesis of YVO_4 crystals in ultra-wide pH range conditions," *Journal of Materials Chemistry*, vol. 13, no. 5, pp. 1223–1228, 2003.

[10] X. Wu, Y. Tao, L. Dong, J. Zhu, and Z. Hu, "Preparation of single-crystalline $NdVO_4$Nanorods, and their emissions in the ultraviolet and blue under ultraviolet excitation," *The Journal of Physical Chemistry B*, vol. 109, no. 23, pp. 11544–11547, 2005.

[11] X. Wu, Y. Tao, C. Mao, D. Liu, and Y. Mao, "In situ hydrothermal synthesis of YVO_4 nanorods and microtubes using (NH_4) $0.5V_2O_5$ nanowires templates," *Journal of Crystal Growth*, vol. 290, no. 1, pp. 207–212, 2006.

[12] A. Huignard, V. Buissette, G. Laurent, T. Gacoin, and J.-P. Boilot, "Synthesis and characterizations of YVO_4: Eu colloids," *Chemistry of Materials*, vol. 14, no. 5, pp. 2264–2269, 2002.

[13] R. G. Banal, Y. Taniyasu, and H. Yamamoto, "Deep-ultraviolet light emission properties of nonpolar M-plane AlGaN quantum wells," *Appllied Physics Letters*, vol. 105, no. 5, Article ID 053104, 2014.

[14] J. H. Huang, J. Deng, Y. G. Cao et al., "Passively mode-locked radially polarized laser based on ceramic Nd:YAG rod," *Optics Express*, vol. 19, pp. 2120–2124, 2011.

[15] A. A. Lagatsky, A. R. Sarmani, C. T. A. Brown et al., "Yb^{3+}-doped YVO_4 crystal for efficient Kerr-lens mode locking in solid-state lasers," *Optics Letters*, vol. 30, no. 23, pp. 3234–3239, 2005.

[16] L. Chen, Y. Liu, and K. Huang, "Hydrothermal synthesis and characterization of YVO_4-based phosphors doped with Eu^{3+} ion," *Materials Research Bulletin*, vol. 41, no. 1, pp. 158–166, 2006.

[17] G. Blasse and A. Bril, "A new phosphor for flying-spot cathode-ray tubes for color television: Yellow-Emitting $Y_3Al_5O_{12}$-Ce^{3+}," *Applied Physics Letters*, vol. 11, no. 2, pp. 53–55, 1967.

[18] H. Wang, O. Odawara, and H. Wada, "Morphology and optical properties of YVO_4: Eu^{3+} nanoparticles fabricated by laser ablation in ethanol," *Applied Surface Science*, vol. 425, pp. 689–695, 2017.

[19] K. Deng, C. Li, S. Huang et al., "Recent progress in near infrared light triggered photodynamic therapy," *Small*, vol. 13, no. 27, Article ID 1702299, 2017.

[20] L. S. Yang, G. S. Li, M. L. Zhao, E. R. Yang, and L. P. Li, "Lattice defect quenching effects on luminescence properties of Eu^{3+}-doped YVO_4 nanoparticles," *Journal of Nanoparticle Research*, vol. 15, 2013.

[21] J. Ruiz-Fuertes, O. Gomis, S. F. León-Luis et al., "Pressure-induced amorphization of YVO_4:Eu^{3+} nanoboxes," *Nanotechnology*, vol. 27, pp. 025701–025708, 2016.

[22] E. R. Yang, G. S. Li, J. Zheng, and C. C. Fu, "Kinetic Control over YVO_4: Eu^{3+} nanoparticles for tailored structure and luminescence properties," *The Journal of Physical Chemistry C*, vol. 118, pp. 3820–3827, 2015.

[23] X. Wu, Y. Tao, C. Song, C. Mao, L. Dong, and J. Zhu, "Morphological control and luminescent properties of YVO_4: Eu nanocrystals," *The Journal of Physical Chemistry B*, vol. 110, no. 32, pp. 15791–15796, 2006.

[24] L. Zhu, J. Li, Q. Li, X. Liu, J. Meng, and X. Cao, "Sonochemical synthesis and photoluminescent property of YVO_4: Eu nanocrystals," *Nanotechnology*, vol. 18, Article ID 055604, 2007.

[25] G. Li, K. Chao, H. Peng, and K. Chen, "Hydrothermal synthesis and characterization of YVO_4 and YVO_4: Eu^{3+} nanobelts and polyhedral micron crystals," *The Journal of Physical Chemistry C*, vol. 112, no. 16, pp. 6228–6231, 2008.